Scripta Materialia 154 (2018) 172–175

Contents lists available at ScienceDirect

Scripta Materialia

journal homepage: www.elsevier.com/locate/scriptamat

Regular article

On the correlation of shear band formation and texture evolution in α-brass during accumulative roll bonding

Marcus Böhme*, Martin F.-X. Wagner

Chemnitz University of Technology, Institute of Materials Science and Engineering, Erfenschlager Str. 73, Chemnitz 09125, Germany

ARTICLE INFO

Article history:
Received 12 March 2018
Received in revised form 21 May 2018
Accepted 25 May 2018
Available online xxxx

Keywords:
Accumulative roll bonding
Brass
Texture
XRD
Shear bands

ABSTRACT

We studied the microstructural evolution of the low stacking fault energy α-brass alloy CuZn15 during accumulative roll bonding (ARB). Most notably, the typical brass-type texture was clearly observed after four ARB passes (approx. 93.8% total thickness reduction), before significant shear localization set in. This observation contradicts the widely accepted idea that shear band formation is a necessary prerequisite for the development of the brass type texture, indicating that the two phenomena, shear banding and development of the brass texture, are only correlated in ARB, and that their order of appearance can be switched depending on experimental parameters.

© 2018 Published by Elsevier Ltd.

It is well-documented that two distinct rolling textures can occur in face-centered cubic (fcc) metals [1-6]. The type of texture developed during cold rolling strongly correlates with the stacking fault energy (SFE) of the metal or alloy. Materials with a high SFE, like aluminum, develop a so-called copper-type texture with prevalent {112}<111> (copper) and {123}<634> (S) texture components [2-4,6]. In contrast, low SFE alloys like α-brass with medium to high zinc contents predominantly show {011}<211> (brass) and {011}<100> (Goss) orientations – appropriately also called brass-type texture [5,6]. Many low SFE materials like Cu-Zn alloys [3-5], Cu-Al alloys [7,8] or pure silver [8,9] form fine deformation twins during the initial stages of plane strain deformation (i.e., during rolling). The tightly packed twin boundaries inhibit conventional dislocation multislip and it is commonly assumed that shear bands are created at large deformations as the only mechanism to accommodate the imposed strains [3,4,7-9]. In fact, nucleation and growth of these shear bands are typically considered to be the main mechanism that facilitates the subsequent development of the brass-type texture components [9-12].

While the correlation (and apparent causality) of shear band formation and brass-type texture evolution has been well documented during conventional rolling, much less is known about their interaction in other processes with a near plane-strain deformation. The accumulative roll bonding (ARB) process, originally proposed by Saito et al. [13], for instance, is an interesting tool to investigate severe plastic deformation in sheet materials. By repeatedly cutting and stacking the material between individual rolling passes, large amounts of plastic strain can be accumulated and ultrafine-grained (UFG) microstructures can be produced while keeping a constant sheet thickness. Nominally, five ARB passes correspond to a von Mises equivalent plastic strain (determined as defined in [13]) of $\varepsilon_{eq} = 4.0$, i.e., to a total thickness reduction of approx. 97%. One advantage of ARB is that the significant amounts of shear strain (i.e., redundant shear strains that primarily occur near the surface) can lead to faster grain size reduction [14]. Compared to conventional rolling, much less has been published on shear banding and texture evolution during ARB, and the literature appears to be partially incomplete. For instance, Pasebani et al. observed brass and Goss as the dominant texture components after three ARB cycles in a 70/30 brass; they discussed shear banding as main cause for the texture transition similar to conventional rolling [15,16]. Chen et al. also reported behavior similar to conventional rolling in pure copper with a {211}<111> copper texture after six ARB cycles [17]. Shaarbaf and Toroghinejad, in contrast, reported the development of a shear type texture in copper after four ARB passes [18]. Finally, to the best of our knowledge only little research has been published on ARB of alloys that can develop either a copper-type or a brass-type texture depending on the experimental conditions, despite the fact that

* Corresponding author.
E-mail addresses: marcus.boehme@mb.tu-chemnitz.de (M. Böhme), martin.wagner@mb.tu-chemnitz.de (M. F.-X. Wagner).

https://doi.org/10.1016/j.scriptamat.2018.05.044
1359-6462/© 2018 Published by Elsevier Ltd.

such investigations may shed more light on the interesting topic of the interaction of shear band formation and texture development. In the present work we therefore study microstructural (via scanning electron microscopy, SEM) and texture evolution (via X-ray diffraction, XRD) of an α-brass with 15 wt% zinc during ARB. This allows for a comparison to well-established results obtained by Leffers et al. for conventional rolling with intermediate thickness reductions [19,5,20]. CuZn15 is of special interest as it shows a dominant brass-type texture after cold rolling although the overall volume of twins formed is only a few percent [5,21].

A commercially available CuZn15 sheet material (obtained from Mecu GmbH, Velbert, Germany; chemical composition in wt%: Cu – 84.2, Zn – 15.66, Ni – 0.045, Pb – 0.023, Sn – 0.013, other – 0.059) with an initial thickness of 2 mm was cut to strips (100mm × 30 mm), rolled down to a thickness of 1 mm and recrystallized at 450 ° C for 30 min. ARB was performed on a laboratory rolling mill with 190 mm roll diameter at a rolling speed of 0.06 m s^{-1} without lubrication. The stacked sheet samples were pre-heated to 473 K before rolling to improve the bonding quality. After each ARB pass, a strip (length 1 cm) was cut from the center of the samples for SEM analysis and XRD texture measurements. The SEM samples were cut in the RD-ND plane, ground and polished with final polishing on a vibratory polisher (Buehler VibroMet 2) using 50 nm alumina suspension. SEM and EBSD investigations were performed with a Zeiss NEON 40 EsB field emitting SEM equipped with a retractable four quadrant backscattered electron detector (QBSD) mounted under the pole piece and an EDAX Digiview III EBSD camera. For XRD texture analysis, samples were cut from the center of the ARB sheets and ground to a depth of approximately 400 μm in the RD-TD plane to reduce the influence of redundant shear strains near the surface. Subsequently, incomplete ($0 \leq \alpha \leq 80°$) {111}, {200} and {220} pole figures were measured with a Siemens D5000 diffractometer in reflection geometry using Cu-K$_\alpha$ radiation and corrected for background. No additional defocussing correction was applied. Crystallographic orientation distribution functions (ODFs) were calculated from these pole figures using the MTEX toolbox [22] for MatLab. We assumed an orthotropic sample symmetry for all samples after this was verified for $N = 3$ to $N = 5$.

The SEM investigations (Fig. 1) show that the material generally exhibits the well-known microstructural deformation mechanisms associated with ARB: we observed both a reduction of grain size with increasing number of passes and mechanical twinning. After four ARB passes ($\varepsilon_{eq} = 3.2$ or 93.8% total thickness reduction), the microstructure is macroscopically homogenous along the rolling direction (Fig. 1a). Heterogeneities/microstructural gradients in the normal direction are a direct result of ARB processing. The distinctive stripe in the center of the micrograph marks the position of the bonding zone that was formed during the fourth ARB pass. The two symmetrically arranged stripes above and below originate from previous ARB passes. Additional inhomogeneities are observed at a much smaller length scale (Fig. 1c) up to three ARB passes. Surrounded by grains that have been refined already to an average subgrain diameter well below 500 nm, there are some significantly larger, residual grains, containing densely packed twins with twin boundaries oriented parallel to the rolling direction (clearly visible as striped patterns in the QBSD micrographs; the twins are expected to be of type {111}<112>). The overall volume fraction of twinned grains remained nearly constant during ARB and was estimated to be below 10%. These microstructural observations are consistent with the low amount of mechanical twins reported by Leffers and Bilde-Sørensen [5] and Christoffersen and Leffers [21] after conventional rolling. It is likely that twinning contributes to stabilization of the few relatively large grains.

It is important to highlight that no shear bands are observed after 4 ARB passes, whereas after the fifth pass ($\varepsilon_{eq} = 4.0$ or 96.9% total reduction), many shear bands that run diagonally through the RD-ND plane with two distinct orientations are visible in the QBSD micrographs as dark stripes (Fig. 1b). The micrograph at higher magnification (Fig. 1d) reveals the complex interaction of the intersecting shear bands. Most interestingly, the two shear bands running from the top left to the bottom right are aligned parallel to each other prior to their intersection with the band running from the top left

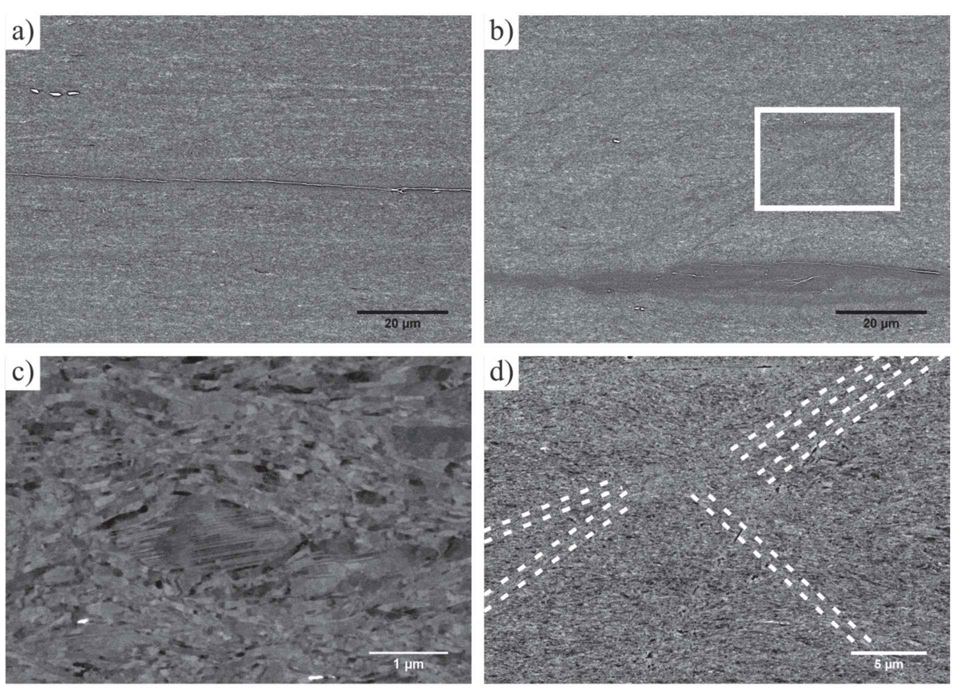

Fig. 1. QBSD electron micrographs taken from the RD-ND plane between ARB passes. The top row shows overview micrographs after (a) 4 and (b) 5 passes. The contrast in these micrographs was inverted to increase the visibility of bonding zones and shear bands. Higher magnification micrographs after (c) 3 and (d) 5 ARB passes are shown in the bottom row without contrast inversion. The white frame in (b) marks the position of the detailed view in (d). Dashed white lines in (d) indicate the orientations of several distinct shear bands.

Download English Version:

https://daneshyari.com/en/article/7910689

Download Persian Version:

https://daneshyari.com/article/7910689

Daneshyari.com